NASA Technical Memorandum 86890

Heat Transfer Results and Operational Characteristics of the NASA Lewis Research Center Hot Section Cascade Test Facility

Herbert J. Gladden, Frederick C. Yeh,
and Dennis L. Fronek
Lewis Research Center
Cleveland, Ohio

Prepared for the
Thirtieth International Gas Turbine Conference and Exhibit
sponsored by the American Society of Mechanical Engineers
Houston, Texas, March 17–21, 1985

NASA

HEAT TRANSFER RESULTS AND OPERATIONAL CHARACTERISTICS OF THE NASA LEWIS RESEARCH CENTER HOT SECTION CASCADE TEST FACILITY

by

Herbert J. Gladden, Frederick C. Yeh, and Dennis L. Fronek
National Aeronautics and Space Administration
Lewis Research Center
Cleveland, Ohio 44135

ABSTRACT

The NASA Lewis Research Center gas turbine hot section test facility has been developed to provide a "real-engine" environment with well known boundary conditions for the aerothermal performance evaluation/verification of computer design codes. The initial aerothermal research data obtained at this facility are presented and the operational characteristics of the facility are discussed. This facility is capable of testing at temperatures and pressures up to 1600 K and 18 atm which corresponds to a vane exit Reynolds number range of 0.5×10^6 to 2.5×10^6 based on vane chord. The component cooling air temperature can be independently modulated between 330 and 700 K providing gas-to-coolant temperature ratios similar to current engine application. Research instrumentation of the test components provide conventional pressure and temperature measurements as well as metal temperatures measured by IR-photography. The primary data acquisition mode is steady state through a 704 channel multiplexer/digitizer. The test facility was configured as an annular cascade of full coverage film cooled vanes for the initial series of research tests. These vanes were tested over a wide range of gas Reynolds number, exit gas Mach number and heat flux levels. The range of test conditions was used to represent both actual operating conditions and similarity state conditions of a gas turbine engine. The results are presented for the aerothermal performance of the facility and the full coverage film cooled vanes.

NOMENCLATURE

C	vane true chord length
g_c	gravitational constant
i	local measurement point
L	total distance along vane surface, on pressure or suction side
P	pressure
P1-P6	measurement locations 1 to 6 on pressure surface
Q/A	heat flux
R	gas constant
Re	Reynolds number
r	radius
S1-S6	measurement locations 1 through 6 on suction surface
SP	measurement at leading edge stagnation point
T	temperature
V/V_{cr}	ratio of local velocity to critical velocity
w	weight flow
X	sum of distances between measurement points
x	surface distance measured from the leading edge stagnation point
Δr	distance between radius at temperature measurement location and vane inner radius
γ	specific heat ratio
η	combustor efficiency
μ	viscosity
ρ	density
φ	cooling effectiveness

Subscripts

c	coolant
cal	calculated
ci	coolant inlet
e	stator exit or station 5
g	gas
in	combustor inlet
meas	measured
o	outside
theo	theoretical
w	metal wall
4,5,6	axial station 4, 5, or 6 (combustor exit, stator exit, or rotor exit)

Supercripts

-	average
'	total

INTRODUCTION

Improved performance of turbojet and turbofan engines is typically accompanied by increased cycle pressure ratio and combustor exit gas temperature. Gas pressure levels of 25 to 30 atm and gas temperatures of 1600 K exist in some current operational engines while pressure levels up to 40 atm with temperatures of 1800 K are anticipated in advanced commercial engines. These continuing increases in the turbine entry gas pressure and temperature of the modern gas turbine

engine and its high development cost put a premium on an accurate initial aerothermal design of the turbine hot section hardware.

The design goals for commercial jet engines include high cycle efficiency, increased durability of the hot section components (lower maintenance costs) and lower operating costs. These goals are contradictory in that high cycle efficiency requires minimizing the cooling air requirements while increased durability requires metal temperatures and temperature gradients to be minimized. An optimum design can only be realized through an improved understanding of the flow field and the heat transfer process in the turbine gas path.

Sophisticated computer design codes are being developed which have the potential of providing the designer with significantly better initial estimates of the flow field and heat load on the hot section components. These codes are being evaluated and verified through low temperature and pressure research in cascades and tunnels. However, by design, these facilities do not model all of the processes that exist in a real engine environment, and therefore, the ability of the design codes to predict the interaction of the various parameters can not be fully evaluated.

The gas turbine hot section test facility at the NASA Lewis Research Center has been developed to provide a "real engine" environment with known boundary conditions. With detailed instrumentation and advanced instrumentation techniques this facility provides the means of verifying the aerothermal performance prediction codes as well as the evaluation of thermal scaling techniques.

This paper presents the initial research test results obtained in the turbine hot section test facility. The test section was configured as an annular cascade for the initial research testing and rig qualification. This facility is currently capable of providing test conditions up to 1600 K and 18 atm. This corresponds to a vane exit Reynolds number range of one-half to two and one-half million. The component cooling air can be independently modulated between 330 and 700 K thus providing gas-to-coolant temperature ratios corresponding to current engine application.

Thermal scaling results are presented by comparing experimental data at constant Reynolds number over a wide range of temperatures and pressures. The aerodynamic performance of the cascade is also presented and compared with cold-air annular cascade tests of solid vanes with the same aerodynamic design. The stability of the facility and repeatability of the data were investigated and the results are also presented.

FACILITY

General Description

A physical layout of the Hot Section Facility (HSF) is shown in the perspective view (Fig. 1(a)). The HSF facility located at NASA Lewis Research Center is a unique facility having fully-automated control of the research rig through an integrated system of minicomputers and programmable controllers. The major components of this facility and how they interface together to provide a real engine environment are shown in the flow diagram (Fig. 1(b)). This facility is discussed in more detail in Ref. 1.

The main air supply system provides air at 10 atm to a nonvitiated preheater. The preheater modulates the air temperature between ambient and 560 K. Through a set of routing valves, two modes of operation can be selected. Utilizing the compressor bypass system, air can be provided to the test rig at 10 atm and up to 560 K. The second mode, compressor-mode, can provide air to the research rig at pressure up to 20 atm and a temperature up to 730 K when utilizing the heat of compression.

The research test rigs (Fig. 1(a)) consist of two independent test stands. a modified turbine test rig (full annular cascade rig) and a combustor test rig. The combustor test rig was used to develop and document the exit temperature profile and efficiency of the heat source for the full annular cascade. Utilizing three pairs of instrumentation rakes (temperature, pressure, and exhaust products) located at the exit of the combustor, the circumferential and radial profiles were documented providing a known input profile for the cascade vane row.

Cascade Configuration

A cross-section of the Hot Section Cascade Rig is shown in Fig. 2. The major components consist of a heat source (combustor), the full annular vane row (containing full coverage film cooled vanes), an exhaust duct line, a quench system (to lower the temperature of the exhaust gas), and the exhaust system.

The vane row consists of 36 full coverage film-cooled (FCFC) stator vanes. The 36 vanes are separated into two groups: 10 tests vanes and 26 slave vanes. The test vane and slave vane cooling air is supplied from two separate manifolds with the flow rates to each manifold independently computer controlled.

FCFC Vane

The stator vane configuration used for these tests was a full coverage film cooled design with an impingement insert to provide augmented coolant-side heat transfer. The vane row hub and tip diameters were 0.432 and 0.508 m, respectively. Both the vane height and chord were 3.81 cm. More detailed geometric data are given in Table I and Ref. 2.

A typical slave vane and test vane are shown in Fig. 3(a). The cooling air supply tube on the tip of the test vane allows cooling air to be supplied from a manifold separate from the slave vane supply. The test vane shown in Fig. 3(a) is in its finished form while the slave vane is shown in a partially finished form.

The stator case is shown partially assembled in Fig. 3(b). The ten test vanes and some instrumentation leads are clearly shown. The cavity directly over the vane row feeds cooling air to the slave vanes while a separate manifold (downstream of the stator row) feeds cooling air to the test vanes. The top dead center position (zero degree) is also noted in the figure. All circumferential locations are measured in a counter clockwise (CCW) direction from this position looking downstream.

Digital Control Center

The operation and data acquisition for the facility are fully automated through an integrated digital minicomputer system called the Digital Control Center (DCC). A programmable controller interfaces with the DCC and provides a back-up to handle the shutdown of the facility in the event of a failure to the DCC. Four minicomputers and their peripherals make-up the DCC (Fig. 4).

The four minicomputers in the DCC are interconnected, however, each computer has a dedicated task. The computers are labeled according to their primary task, e.g., Input, Control, Operation, and Research computer. The computers and their peripherals are powered by a 30 kW uninterruptable power supply to prevent loss of power while the test is in progress.

The Input computer is the DCC's main interface with the test rig through an analog to digital convertor and multiplexer. Almost all analog signals, e.g.,

strain gages, pressure transducers, temperatures, and position signals enter the DCC through the multiplexer. The multiplexer is a 704 channel (expandable to 1024) amplifier-per-channel digitizer with mixed ranges between 5 mV and 10 V full scale. Calibration voltages can be switched into each channel prior to a test run, thus, verifying proper operation of the system. The main task of the Input computer is to act as a data gathering buffer and intermachine communications buffer.

The Control computer's task is to control 19 highly interactive process variables at update rates of 20 to 150 times/second. This computer has perhaps the most demanding task of the DCC because of the large number of control loops that must be serviced and the speed at which they must be serviced. The Control computer performs the task of 19 separate process controllers.

The third computer, the Operations computer, provides the communications link and interface with the test rig operator. Its primary functions are to provide the operator with control loop status information and health information on the test hardware. All test conditions are prestored in the Operations computer prior to a test run. These set-points are passed to the Control computer when the operator requests a change in conditions. The DCC has the capability to modify the set-points on-line through the Setpoint Entry Keyboard. The health of the hardware is constantly monitored by the Operations computer during a test, and corrective action is automatically taken by the computer if a major limit violation occurs. An example of corrective action might be to turn off the combustor because of an over-temperature.

Research Data System

The fourth computer of the DCC is the Research computer. Its dedicated task is to gather large volumes of research data. The Research computer provides, through cathode ray tube (CRT) displays in almost real time, information on the progress of the experiment. The Research computer acquires the raw data from the Input computer which is then converted to engineering units and calculated values for display.

The Research computer also controls the data gathering process on command of the research engineer. During the data taking cycle, the Research computer prepositions the radial probes, records and stores the raw data, increments the probes to a new position and repeats the process. This is repeated until the data cycle is complete. The raw data is then converted to engineering units, packaged, tagged with a unique number and transferred to the NASA Lewis Research Center's Central Data Collector for permanent storage.

The Data Collector is linked to a larger host computer. This computer is used to further process the data, solving more complex and time consuming equations, e.g., graphics. A return link back to the Hot Section Facility provides the graphics data for viewing on CRT displays.

Instrumentation

Research instrumentation in the HSF is primarily the conventional steady state pressure and temperature measurements. In addition to the conventional transducer per channel pressure measurement, the HSF uses a pressure measuring system that multiplexes the pneumatic signals. This system uses a single transducer to measure 48 pressure channels. Six of the pressure channels are used for calibration. The Cascade rig has three of these systems providing 126 pressure measurements.

A summary of the Cascade Research instrumentation is shown on Fig. 5(a). Gas path conditions (e.g., temperature and pressure) are monitored and recorded at axial stations 4, 5, and 6. The cooling air flow to each of the cooled components is weight flow controlled and measured by venturis in each of the supply lines. Both cooling air temperatures and pressures are measured in the internal manifolds of each cooling air system. The vanes have thermocouples and pressure sensing tubes to sense gas stream conditions, gas-side metal temperatures, and cooling-air side pressures and temperatures.

Stations 4 and 6 have three fixed probe ports each for mounting radially-actuated water cooled probes. Radial gas-path surveys of both temperature and pressure are recorded from vane hub to tip. Station 4 can also utilize an optical probe for infrared photography for surface temperature mapping of the vanes. The infrared data recording and data reduction procedure is discussed in Ref. 3.

A cross-sectional schematic of the vane airfoil is shown in Fig. 5(b). Also shown is a composite summary of instrument locations on the airfoil. The locations shown in Fig. 5(b) represent either metal temperature or static pressure measurements. And, because each airfoil could accommodate only a limited number of instrument grooves, the temperature or pressure distributions reported are composed of measurements from several airfoils in the test vane sector of the annulus.

ANALYTICAL PROCEDURES

Gas Temperature Profile

The combustor exit radial gas total temperature profile was obtained by averaging temperatures from two traversing probes. The third traversing probe was used to measure gas total pressure. The probes were located one vane chord in front of the cascade vane row at station 4. Data were taken at five specific radial steps from vane hub to vane tip. An average radial total temperature profile and an overall average gas total temperature were determined from these measurements.

The average gas temperature, as obtained from two traversing probes, is not representative of the true average combustor exit temperature since two radial profiles from the circumference are not sufficient to define actual total temperature. To alleviate this problem, a theoretical gas temperature, $T_{g,theo}$, was calculated, based on fuel/air ratio, combustion air inlet temperature, measured total and static pressures, inlet temperature, and enthalpy for the fuel (4). A combustor efficiency was then applied to the theoretical temperature to obtain the true combustor exit total temperature. The combustor efficiency is obtained from a set of curves generated from experiments on a similar and extensively instrumented research combustor in a Combustor Research Facility (5).

The temperature correction which takes into account the combustor efficiency has the following form.

$$\bar{T}'_{g,cal} = \eta(T'_{g,theo} - T'_{in}) + T'_{in} \qquad (1)$$

where η is the combustion efficiency.

A radial profile was imposed on the calculated total temperature by using the ratio of the measured radial temperature to the average measured temperature.

$$T'(r)_{g,cal} = \frac{\bar{T}'_{g,cal}}{\bar{T}'_{g,meas}} T'(r)_{g,meas} \quad (2)$$

Cooling Effectiveness

Cooling effectiveness, φ, is used to compare the vane performance and thermal scaling at various combustor exit temperatures, coolant flow rates, Mach numbers and Reynolds numbers. The local cooling effectiveness, φ, is defined as:

$$\varphi(i) = \frac{T'(r)_{g,cal} - T(i)_w}{T'(r)_{g,cal} - T_{ci}} \quad (3)$$

where $T(i)_w$ refers to local metal temperature on the test vane surface, and $T'(r)_{g,cal}$ is the calculated total gas temperature at a specific radial location. An average cooling effectiveness, $\bar{\varphi}$, is also calculated, using in place of $T(i)_w$ an averaged metal temperature $\bar{T}_w$, defined as:

$$\bar{T}_w = \sum_{i=2}^{13} \frac{[T(i)_w + T(i-1)_w][x(i) - x(i-1)]}{2X} \quad (4)$$

where (i) refers to a specific temperature measurement point on the vane surface, x(i) the distance along the vane surface measured from the leading edge stagnation point, and X the sum of distances between measurement points.

Reynolds Number

The exit gas Reynolds number is based on the vane row inlet total temperature and pressure, the vane row exit static pressure and the vane true chord length. The gas properties are based on exit static gas temperature derived from the exit static-to-inlet total pressure ratio.

$$Re = \frac{(\rho v)_e C}{\mu} \quad (5)$$

where

$$(\rho v)_e = P'_4 \left(\frac{P_5}{P'_4}\right)^{(2\gamma-1)/\gamma} \left[\frac{2\gamma}{\gamma - 1} \frac{g_c}{RT'_{g,cal}} \left(1 - \left(\frac{P_5}{P'_4}\right)^{(\gamma-1)/\gamma}\right)\right]^{1/2}$$

Critical Velocity Ratio

The exit critical velocity ratio, like the Reynolds number, is based on the vane row exit static pressures and the vane row inlet total pressure.

$$\left(V/V_{cr}\right)_e = \left[\frac{\gamma + 1}{\gamma - 1}\left(1 - \left(\frac{P_5}{P'_4}\right)^{(\gamma-1)/\gamma}\right)\right]^{1/2} \quad (6)$$

EXPERIMENTAL PROCEDURE

There were two basic modes of facility operation: 10- and 20-atm. Within each mode the research rig was operated with the combustor operating (burning) or without combustor operation (isothermal). The research objectives were to investigate the aerothermal performance of this cascade over a range of Reynolds numbers, and at a constant Reynolds number, over a range of combustor exit temperatures and pressures. The various operating modes of this facility permit a great deal of flexibility in setting operating conditions. This flexibility is shown in Fig. 6 and Table II.

The gas conditions were established by setting the combustor inlet total pressure, the vane exit outer radius static pressure, and the combustor fuel/air ratio through predetermined input values stored in the operations computer. The coolant flow rate and temperature were varied systematically at fixed gas conditions either through predetermined input values or through the "set-point entry panel." The vane row exit critical velocity ratio was also varied systematically by discrete changes in the exit static pressure.

RESULTS AND DISCUSSION

The results of this investigation are summarized in this section. Typical boundary condition measurements are presented and then the thermal scaling and aerodynamic performance results are discussed. The infrared temperature data capabilities of this facility are presented. Finally, the operating stability of the facility, and the data repeatability are presented and discussed.

Boundary Conditions

The combustor exit (cascade inlet) and stator row exit gas flow conditions are important to the evaluation of research results. In addition, they can be used to compare rig performance with the design goals. The gas total temperature profile at station 4 is shown in Fig. 7. Measured temperature data from the cascade tests are compared with the results of the combustor development tests conducted at similar conditions. The combustor test data represent a complete circumferential and radial survey of the combustor exit plane (5).

Figure 7(a) shows the radial total temperature profile measured by the two traversing probes at station 4. An average radial total temperature profile and a maximum total temperature profile obtained from the combustor development tests (unpublished) are also shown in the figure. In addition, the calculated average gas temperature for the cascade test conditions is shown by the dashed line. The calculated average gas temperature (Eq. (1)) appears to represent that obtained in the combustor development tests. In addition, the measured temperature profiles correspond reasonably well to the maximum temperature profile obtained during the combustor development tests. Therefore, the use of a radial profile imposed on the calculated average gas temperature (Eq. (2)) was considered appropriate for subsequent data analysis.

The pattern factor for the combustor development tests was approximately 0.35. However, the circumferential temperature distribution, as shown in Fig. 7(b) by a local pattern factor distribution (unpublished data) is relatively uniform. The local hot spots occur in three small discrete locations. The circumferential average total temperature at the mean radius was 1620 K with a standard deviation of 63 K.

The combustor exit total pressure as measured by the radially traversed probe was essentially constant. Inner radius and outer radius static pressure measurements were constant indicating the vane row inlet critical velocity ratio was also constant, both radially and circumferentially, at the nominal design value of 0.23.

The cascade exit total conditions could not be measured accurately because the probes were not designed for the large tangential component at the stator exit. However, based on the outer radius static pressure measurements and the combustor exit total pressure, the critical velocity ratio at the outer radius compared well with the design value of 0.728. The inner radius static pressure measurements also indicated the velocity ratio compared well with the design value of 0.834.

Thermal Scaling

During the development of an engine the turbine components are frequently tested at reduced temperature and pressure in cascades and tunnels to verify the heat transfer design. There has been a concern for the validity of these data and whether the thermal scaling laws are sufficiently satisfied between the rig tests and the actual engine. Data were taken over a wide range of temperatures and pressures in both isothermal (nonburning) and burning mode to investigate the thermal scaling phenomena. The primary parameters held constant were Reynolds number and Mach number. The results are shown in Fig. 8. A midspan average cooling effectiveness parameter, $\overline{\varphi}$, for the full coverage film cooled vane is shown as a function of the coolant-to-gas flow ratio. The gas total temperature used in the effectiveness calculation was the mean radius value obtained from Eq. (2).

The lowest Reynolds number data taken (0.5×10^6) are presented in Fig. 8(a). Two gas total temperature levels for the "burning mode" are shown. A trend is shown by these data where the higher gas temperature data (case 8) have a lower cooling effectiveness compared with the lower gas temperature data (case 7). This difference in cooling effectiveness values is about 0.02 at a coolant-to-gas flow ratio of 0.113.

The data shown in Fig. 8(b) represents a higher Reynolds number (1.25×10^6) as well as both "burning" and "isothermal" modes of testing. These data are characteristic of both engine operation (high gas temperature) and rig tests (low gas temperature). These data show a trend similar to the data in Fig. 8(a). That is, the low gas temperature data (rig tests) have a slightly higher cooling effectiveness when compared to higher gas temperature data (engine conditions). The difference in cooling effectiveness values is about 0.02 at a coolant-to-gas flow ratio of 0.11.

Even though a trend is shown by the data of Figs. 8(a) and (b) the differences are small. The estimated experimental error for $\overline{\varphi}$ is ±0.9 percent for the "isothermal mode" data and ±1.7 percent for the "burning mode" data. This level of error could not reverse the data trend shown but could enhance the cooling effectiveness differences.

Reference 6 predicts up to 0.04 increase in cooling effectiveness from engine conditions to lower temperature rig test conditions. This phenomenon was shown to result from the inability to thermally scale the material thermal conductivity. This trend is shown by both Reynolds number data sets. It can be concluded from these data and Ref. 6 that low temperature rig tests are somewhat optimistic in predicting the cooling performance of a design prototype operating at engine conditions.

The highest Reynolds number data taken are shown in Fig. 8(c). The primary observation is that at the high blowing rates of these tests the cooling effectiveness was not affected by an increased heat flux (Reynolds number). These results are also shown in Fig. 8(d) where constant gas temperature cooling effectiveness data are compared for Reynolds numbers covering a range of 0.5×10^6, 1.25×10^6, and 1.90×10^6. Assuming that the heat flux is proportional to $(Re)^{0.8}$ then the data shown in Fig. 8(d) represents a range of heat flux of 2.9 to one. The good agreement of these data indicate that the flow regime is unchanged (probably turbulent) and that the level of heat flux is not an independent function.

Aerodynamic Performance

The aerodynamic performance of the full coverage film cooled cascade is characterized by the surface static pressure distribution shown in Fig. 9(a). Data are plotted for three different exit critical velocity ratios (design, less than and greater than design). Also shown is the unblown design pressure distribution for this airfoil reported in Ref. 7. The pressure distribution on the pressure surface compares favorably with the design objective. However, the pressure distribution on the suction surface trailing edge was about 7 percent higher than the design values. This indicates that the gas stream was not accelerated to desired velocity.

The total mass flow through the cascade is also important to the overall performance of the stator (and subsequent turbine stage). When full or partial film cooling is used in the stator design one effect of the coolant is to reduce the primary gas flow through the combustor. This effect is shown in Fig. 9(b). The primary-to-total gas flow ratio is shown as a function of the coolant-to-primary flow where the total flow is the sum of the primary and the coolant. The data reported herein follows the same trends as that reported in Ref. 8. Some of Ref. 8 data have been included for comparison. These results show the same trend as Ref. 8 even though these tests were conducted at substantially higher coolant blowing rates. The primary effect of injecting coolant into the gas stream upstream of the stator vane throat is to create blockage and reduce the primary flow through the combustor.

Airfoil Temperature

A thermal image of an airfoil leading edge and pressure surface are shown in Fig. 10. The gray tones represent the temperature of the airfoil through its thermal energy output. The lightest regions are high temperature while the dark regions are cooler. The procedures for recording and interpreting thermal image is discussed in Ref. 3. The gray tones in the figure indicate a hot leading edge and a relatively uniform and lower temperature on the pressure surface. The pattern of dark spots on the leading edge of vane 3 are the film cooling holes.

Facility Operational Characteristics

The operating characteristics and, in particular, the stability of automatic controls and the repeatability of the data have been of concern during the development of this facility. During qualification tests attention was focused on the 20 atm mode of testing when some air flow instability was noted. Modifications of the facility and the controls have improved the situation. Flow stability can be shown by plotting the ratio of the coolant flow and the primary flow with time. The phase shift between these systems should amplify the instability at discrete times. The data shown in Fig. 11(a), taken over a 1 min time period during 20-atm mode operation, do not show any significant flow instability. The majority of the data fall within the 95 percent uncertainty band.

The data repeatability is shown in Fig. 11(b). The average cooling effectiveness was determined for several data points taken at fixed conditions over a period of about 30 min. Each data point required about

1.5 min to record. Both 10- and 20-atm mode of operation were studied. The data for two sets of conditions show a high degree of repeatability. However, at the maximum pressure conditions of the 20-atm mode the data shows some nonrepeatability in the coolant to gas flow ratio (case 6 and case 12, Fig. 11(b)). The facility was operating at essentially full flow conditions with control valves at their upper limit. In general, the operational stability of the facility is marginally acceptable.

CONCLUDING REMARKS

The initial results of research testing in the NASA Lewis Research Center turbine hot section facility are presented. The thermal scaling results show that cooling effectiveness data taken at low temperature rig conditions are somewhat optimistic when used to predict cooling performance at engine conditions. As the heat load is increased by increasing Reynolds number at a constant gas temperature the coolant effectiveness is not affected because of the high blowing rates. The critical velocity ratio distribution (based on the pressure distribution) around the stator airfoil is comparable with the design distribution with the exception of the suction surface trailing edge. The velocity ratio in this region is about 7 percent less than design. However, the inner radius exit velocity ratio and the outer radius velocity ratio compared well with the design values. In the 10-atm mode of operation the facility is very stable and the data repeatability is good. The facility operational stability in the 20-atm mode shows some degradation compared with the 10-atm mode. This, in turn, has an adverse impact on the repeatability of the data particularly near the maximum pressure level. However, the facility operating stability in the 20-atm mode is marginally acceptable.

REFERENCES

1. Cochran, R.P., Norris, J.W., and Jones, R.E., "A High-Pressure, High-Temperature Combustor and Turbine-Cooling Test Facility," ASME Paper 76-WA/GT-4, Dec. 1976.

2. Moffitt, T.P. and Whitney, W.J., "Aerodynamic Effect of a Honeycomb Rotor Tip Shroud on a 50.8 Centimeter-Tip-Diameter Core Turbine," NASA TP-2112, Jan. 1983.

3. Pollack, F.G., and Cochran, R.P., "Temperature and Pressure Measurement Techniques for an Advanced Turbine Test Facility," Measurement Methods in Rotating Components of Turbomachinery, B. Lakshminarayana, and P. Runstadler, Jr., eds., ASME, 1980, pp. 319-326.

4. Svehla, R.A. and McBride, B.J., "Fortran IV Computer Program for Calculation of Thermodynamic and Transport Properties of Complex Chemical Systems," NASA TN-D-7056, 1973.

5. Wear, J.D., et al., "Preliminary Tests of an Advanced High-Temperature Combustion System," NASA TP-2203, 1983.

6. Gladden, H.J., "Extension of Similarity Test Procedures to Cooled Engine Components With Insulating Ceramic Coatings," NASA TP-1615, 1980.

7. Whitney, W.J., et al., "Cold-Air Investigation of a Turbine for High-Temperature-Engine Application. I. Turbine Design and Overall Stator Performance," NASA TN-D-3751, 1967.

8. Stabe, R.G., and Kline, J.F., "Aerodynamic Performance of a Fully Film Cooled Core Turbine Vane Tested with Cold Air in a Two-Dimensional Cascade," NASA TM-X-3177, 1975.

TABLE I. - STATOR VANE GEOMETRY

Mean diameter, cm	46.99
Vane height, cm	3.81
Axial chord, cm	3.81
Axial solidity	0.929
Aspect ratio	1.000
Number of vanes	36
Leading edge radius, cm	0.508
Trailing edge radius, cm	0.089

TABLE II. - HSF CASCADE RESEARCH CONDITIONS

Case	Combustor exit, station 4			Coolant	Exit, station 5		Mode of operation
	Temperature, K	Pressure, atm	V/V_{cr}	Temperature, K	V/V_{cr}, mean radius	Reynolds number	
ISOTHERMAL MODE							
1	500	5.1	0.23	320	0.775	1.25×10^6	10 atm
2	500	6.5	↓	↓	↓	1.90×10^6	10 atm
3	500	8.5				2.50×10^6	10 atm
4	700	4.9				1.25×10^6	20 atm
5	700	7.4				1.90×10^6	20 atm
6	700	9.5				2.50×10^6	20 atm
BURNING MODE							
7	1300	4.2	0.23	430	0.775	0.5×10^6	10 atm
8	1535	5.0	↓	500	.775	0.5×10^6	10 atm
9	945	10.8		320	.71-.83	1.90×10^6	20 atm
10	1165	9.0		390	.72-.80	1.25×10^6	↓
11	1500	11.7		500	.775	1.25×10^6	
12	1500	17.7		500	.775	1.90×10^6	

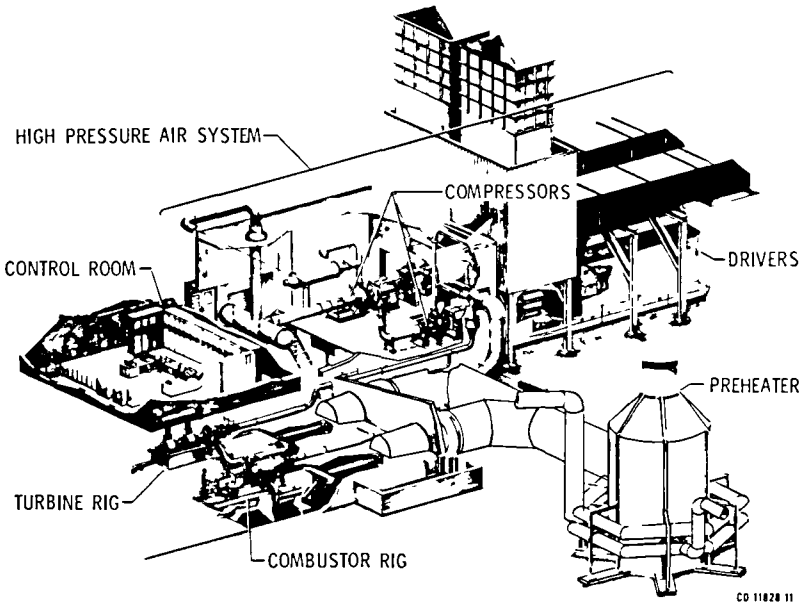

(a) Perspective view.

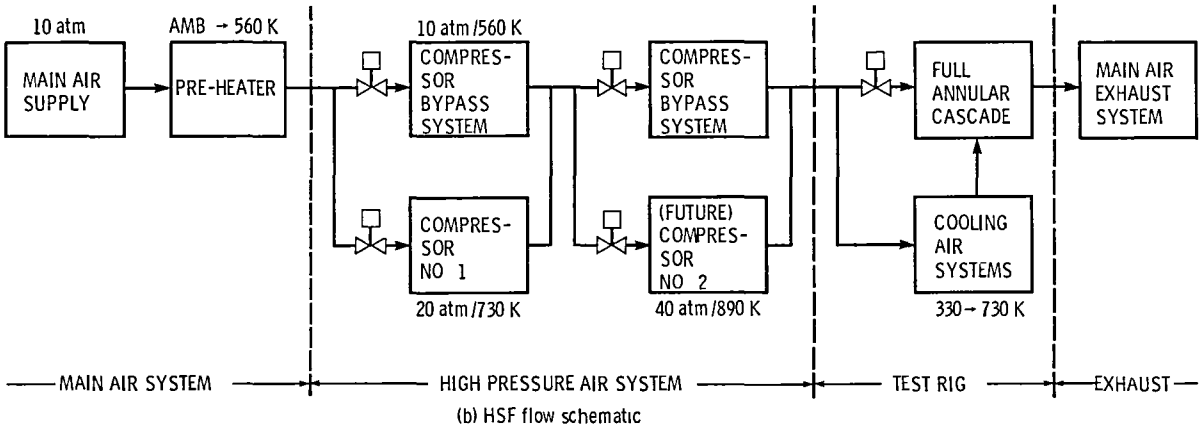

(b) HSF flow schematic

Figure 1. - Hot section test facility.

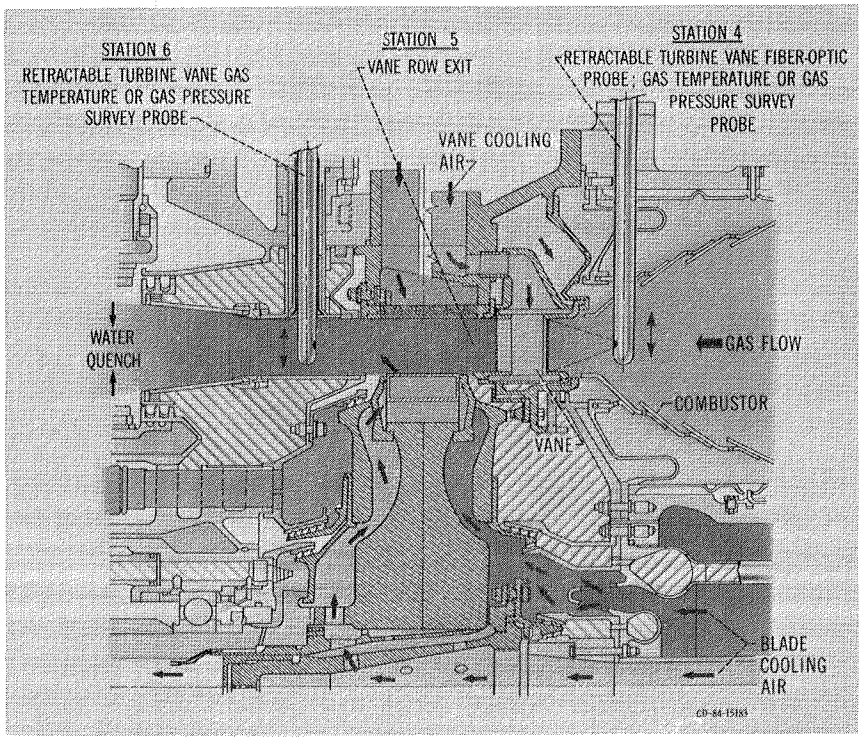

Figure 2. - Cascade schematic cross-section of the combustor and the cascade vane row.

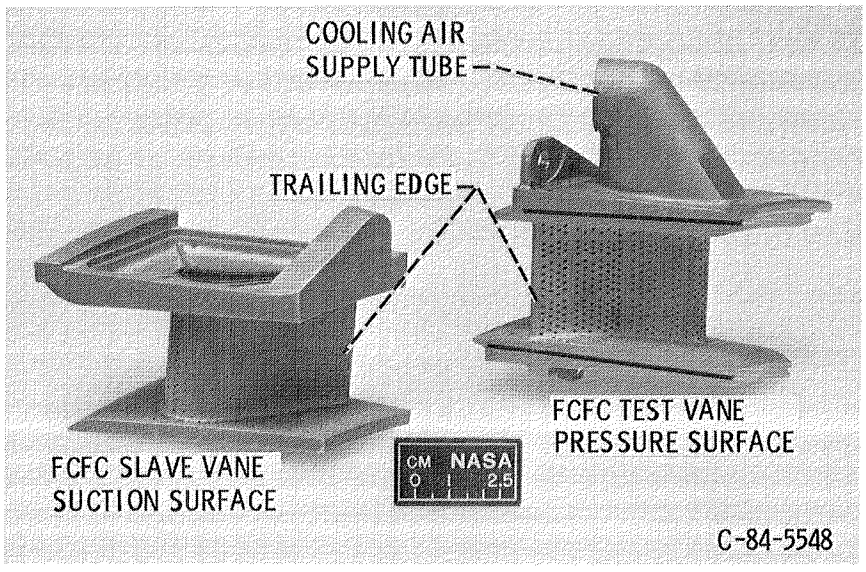

(a) The slave vane is shown in a partially machined form while the test vane is shown in finished form.

Figure 3. - Full coverage film cooled vanes for the Hot Section Facility cascade rig.

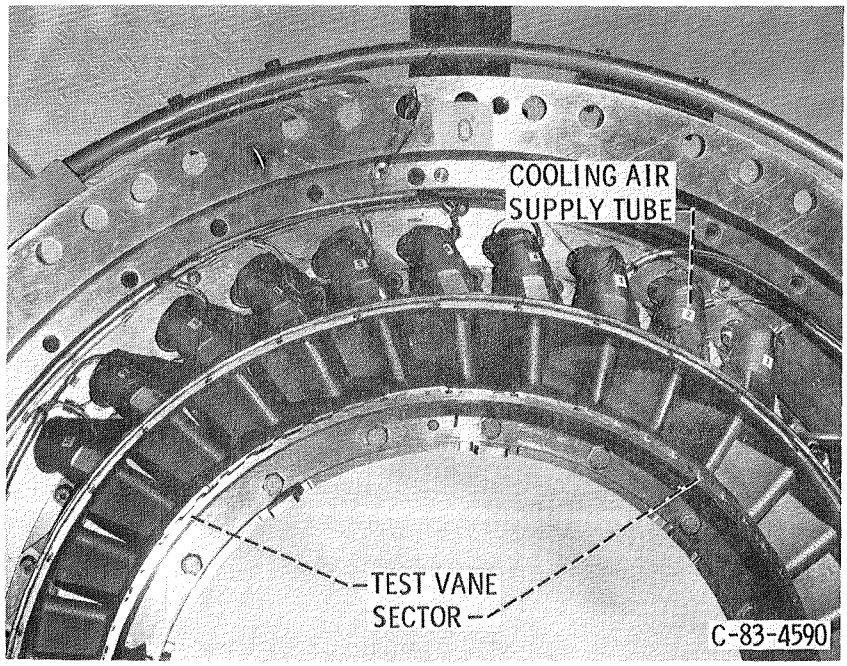

(b) Partial assembly of FCFC stator case showing test vane sector.
Figure 3. - Concluded.

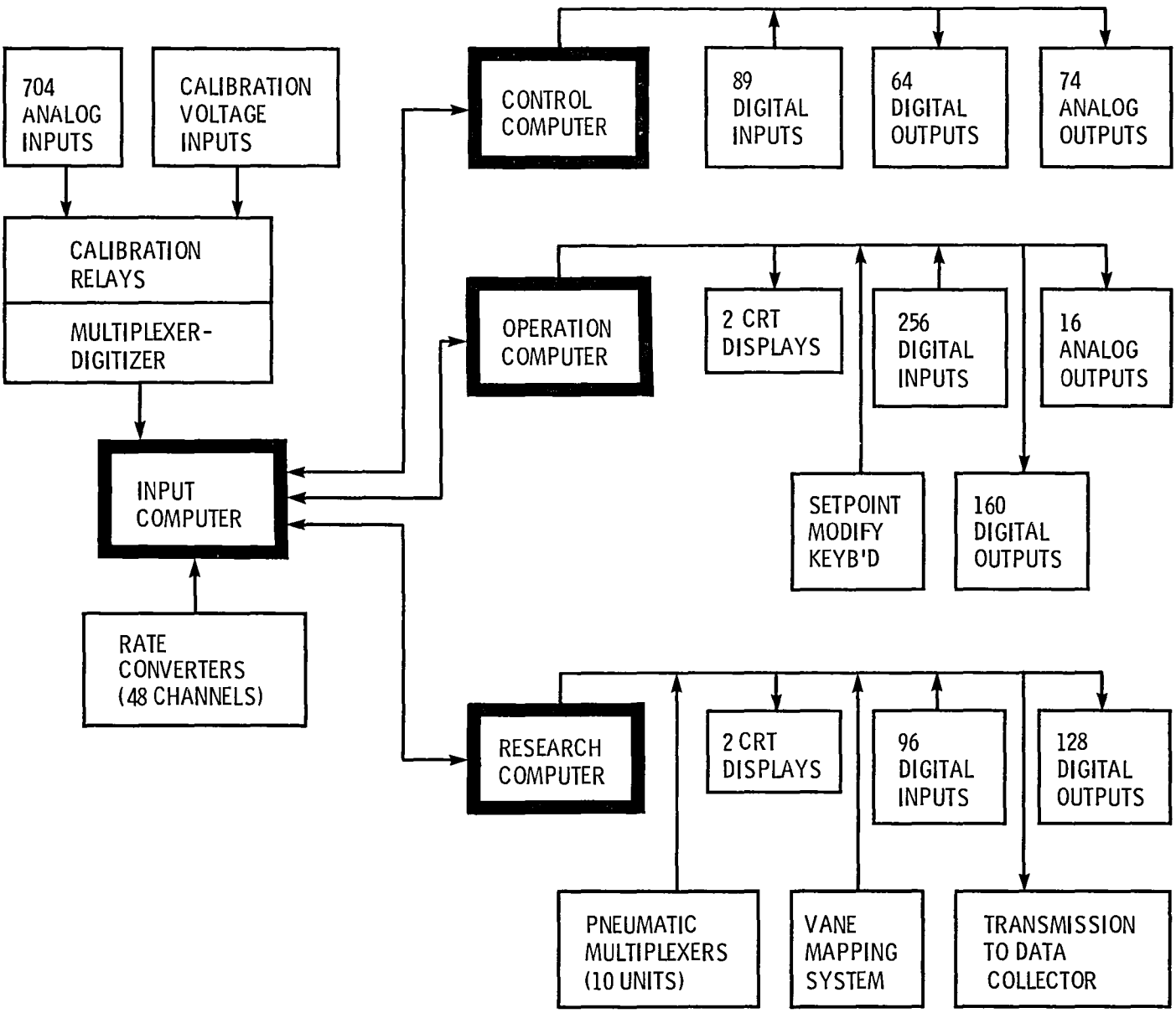

Figure 4. - Schematic of Digital Control Center (DCC).

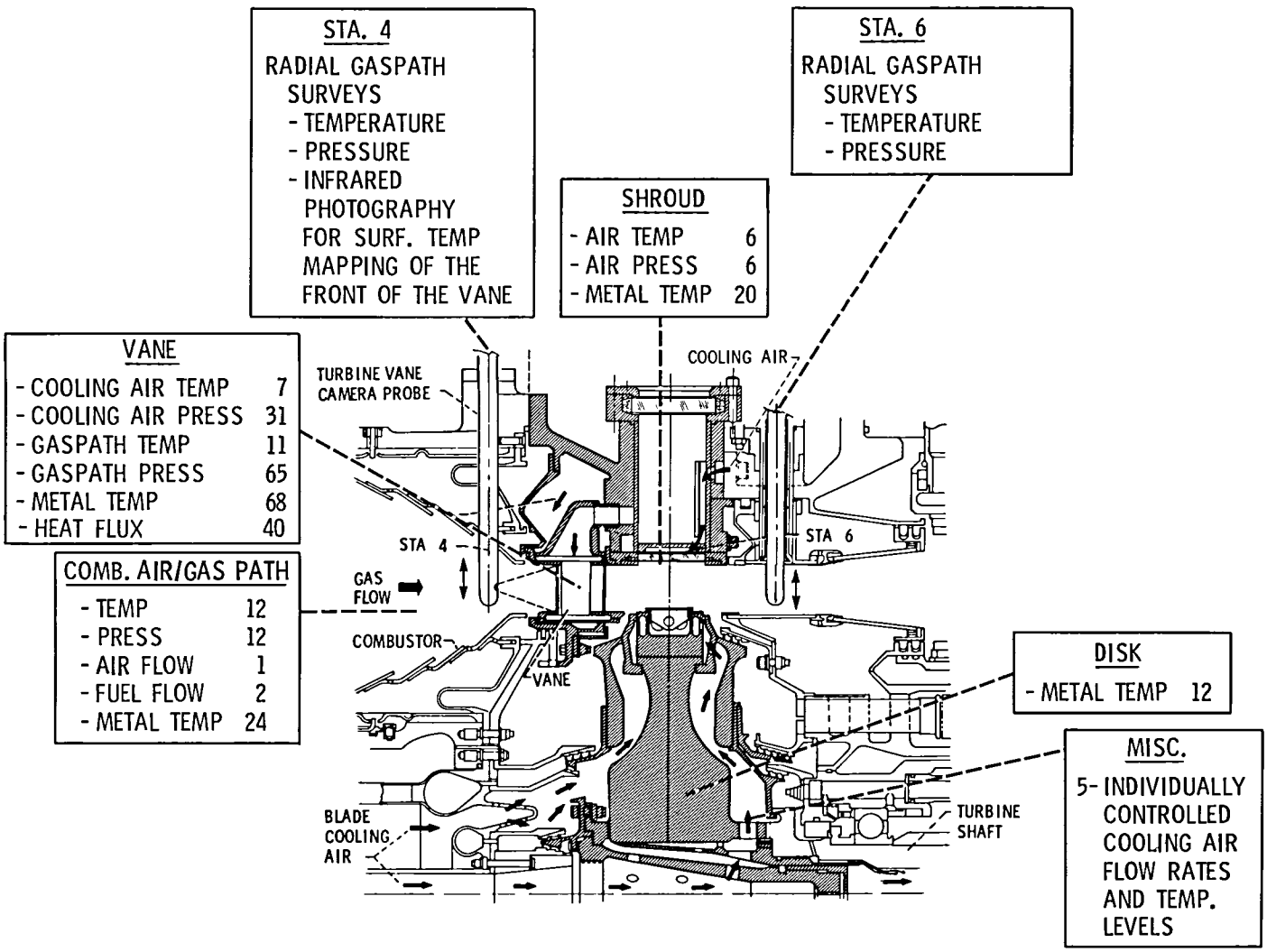

(a) Summary of rig instrumentation.

CD-81-12711

Figure 5. - HSF cascade research instrumentation.

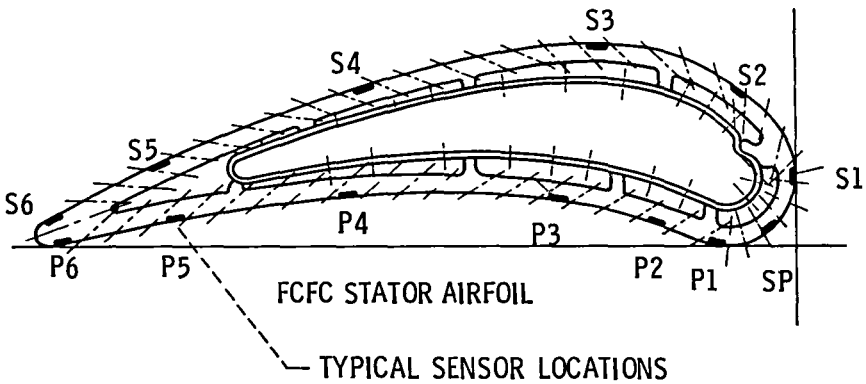

SUCTION SURFACE		PRESSURE SURFACE	
SENSOR	x/L	SENSOR	x/L
SP	0.0		
S1	.067	P1	0.083
S2	.188	P2	.174
S3	.346	P3	.314
S4	.612	P4	.587
S5	.836	P5	.826
S6	.972	P6	.973

(b) Full coverage film cooled vane cross-section showing typical composite of instrumentation.

Figure 5. - Concluded.

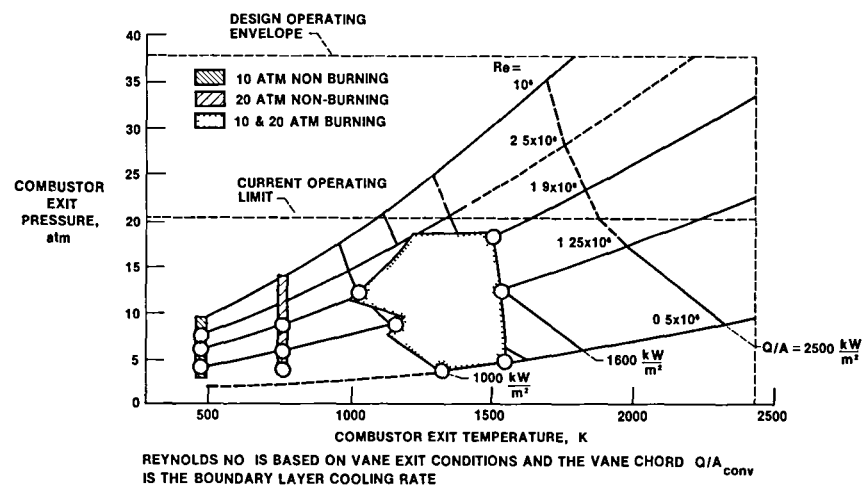

Figure 6. - Cascade rig simulation of real engine operating conditions.

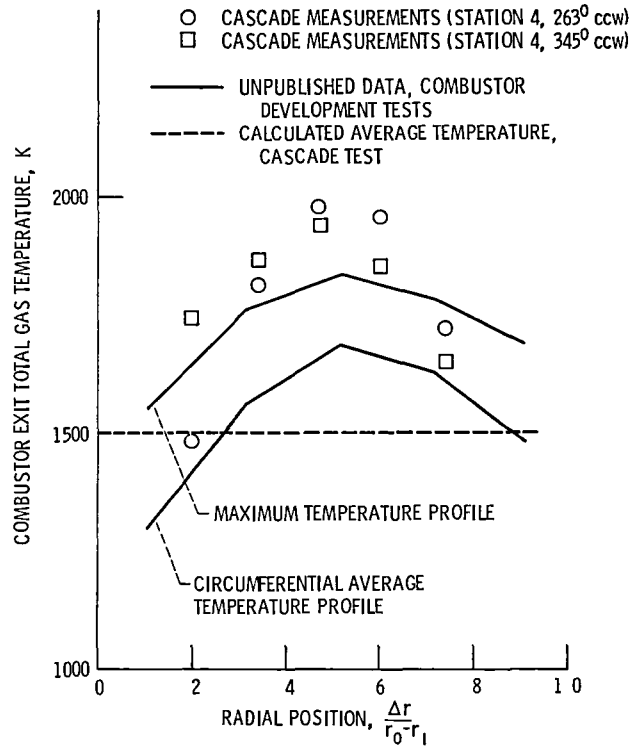

(a) Two circumferential locations are compared with unpublished data from combustor development tests (case 11).

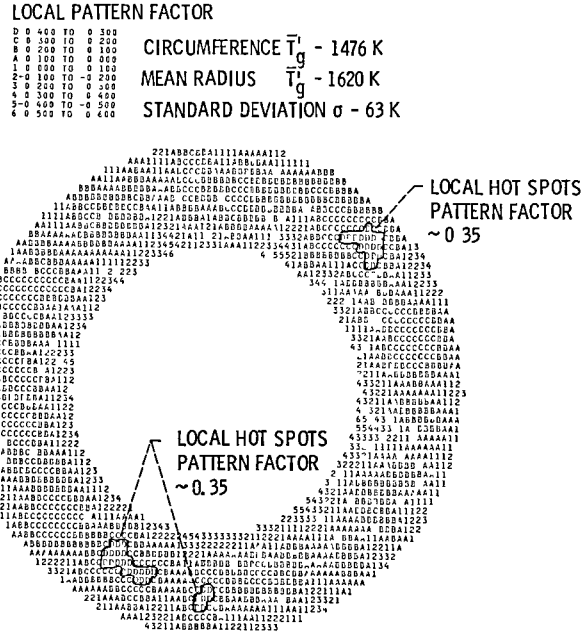

(b) Circumferential distribution of local pattern factor from combustor development tests Conditions similar to case 11 The hot spots are highlighted

Figure 7 - Typical gas total temperature profile at station 4 (combustor exit)

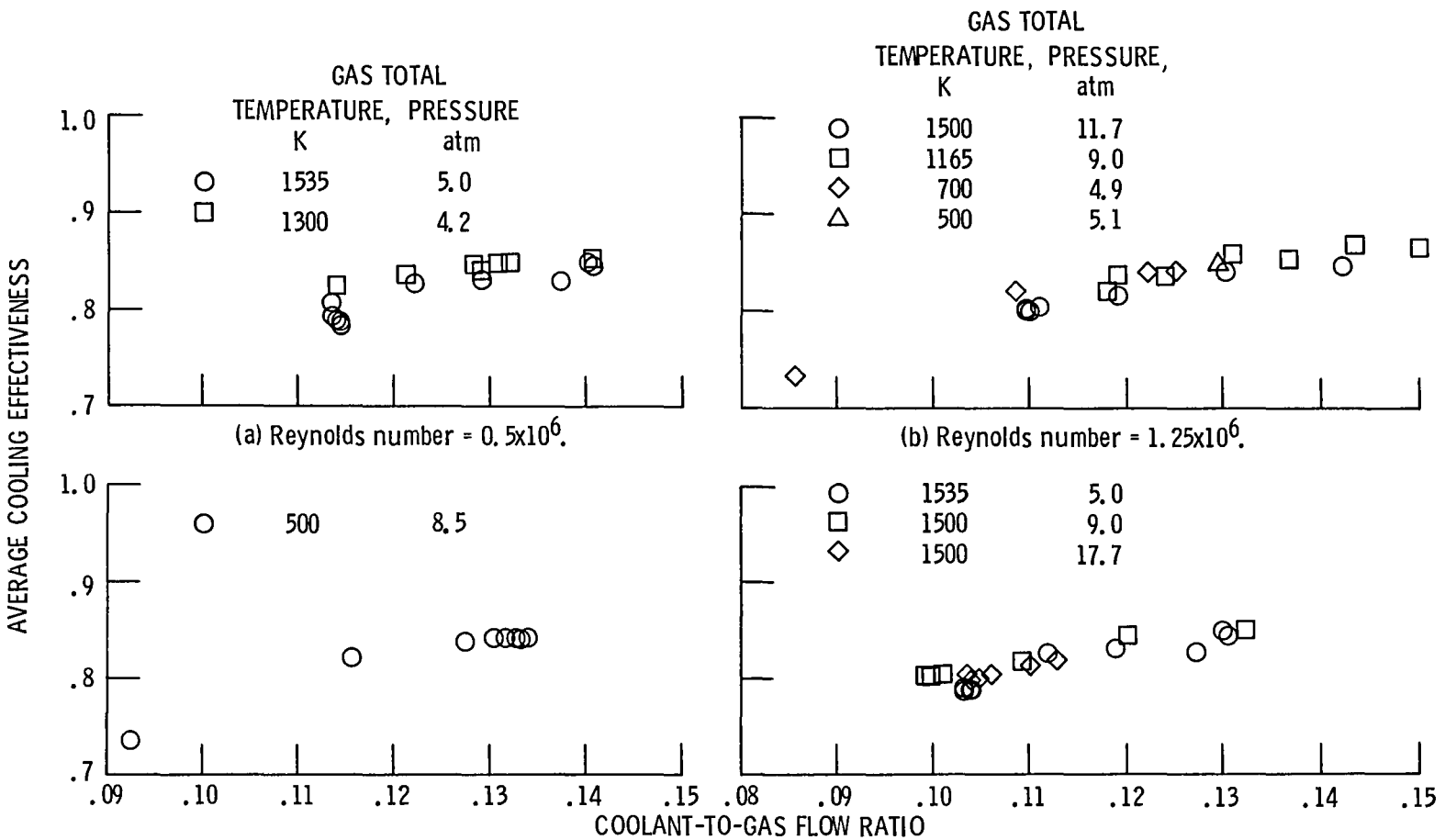

(a) Reynolds number = 0.5×10^6.

(b) Reynolds number = 1.25×10^6.

(c) Reynolds number = 2.5×10^6.

(d) Constant gas temperature = 1500 K.

Figure 8. - Thermal scaling results from the full coverage film cooled vane cascade tests.

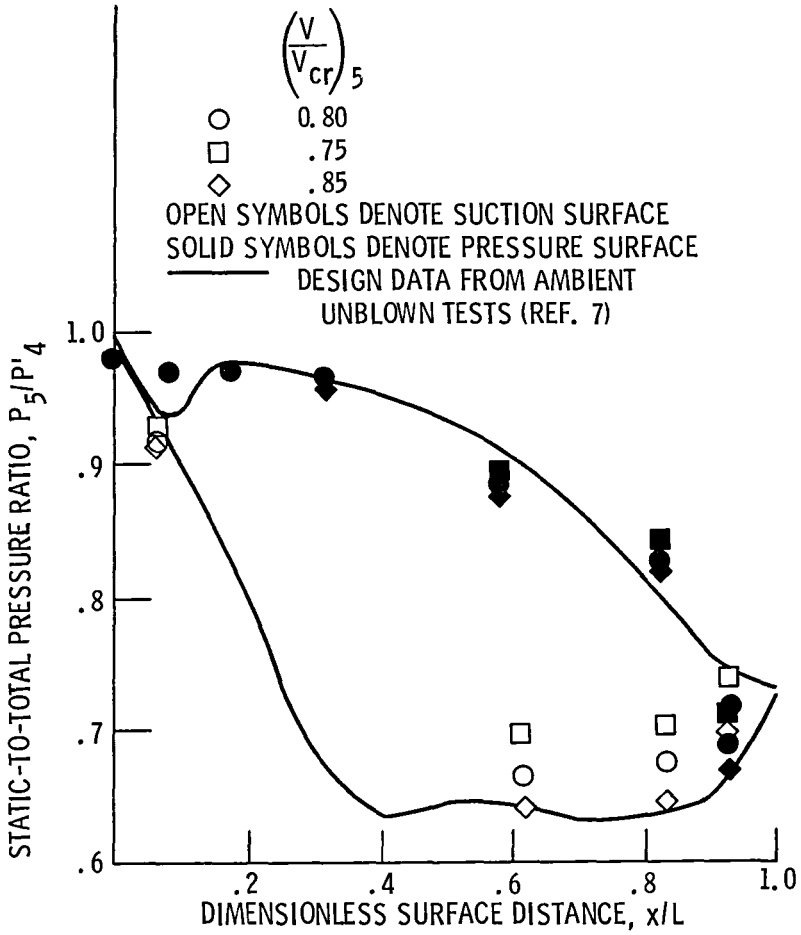

(a) Surface static-to-total pressure distribution variation with exit critical velocity ratio, 1.90×10^6 Reynolds number.

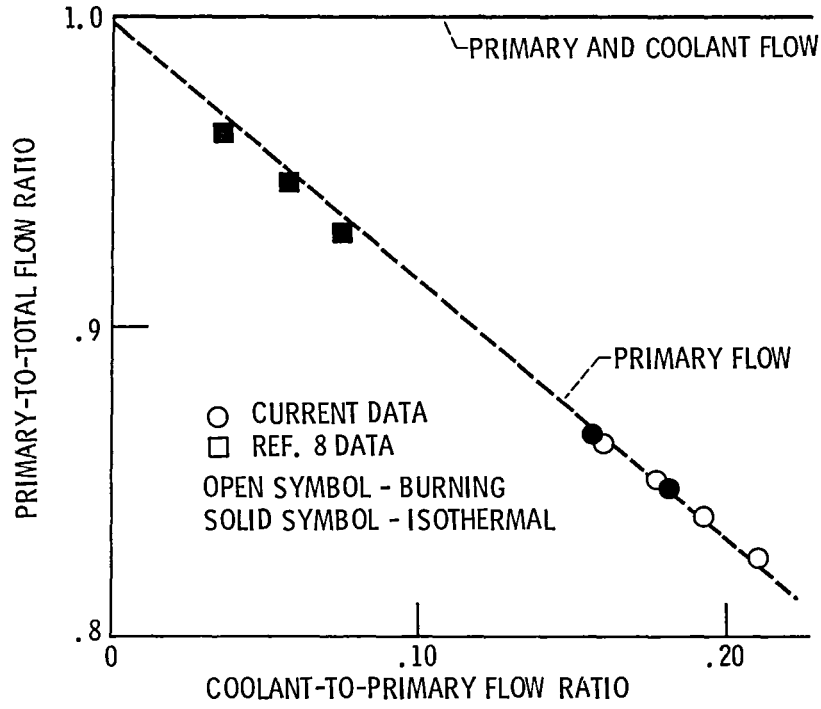

(b) Reduction of primary flow with increased coolant.

Figure 9. - Stator vane aerodynamic performance.

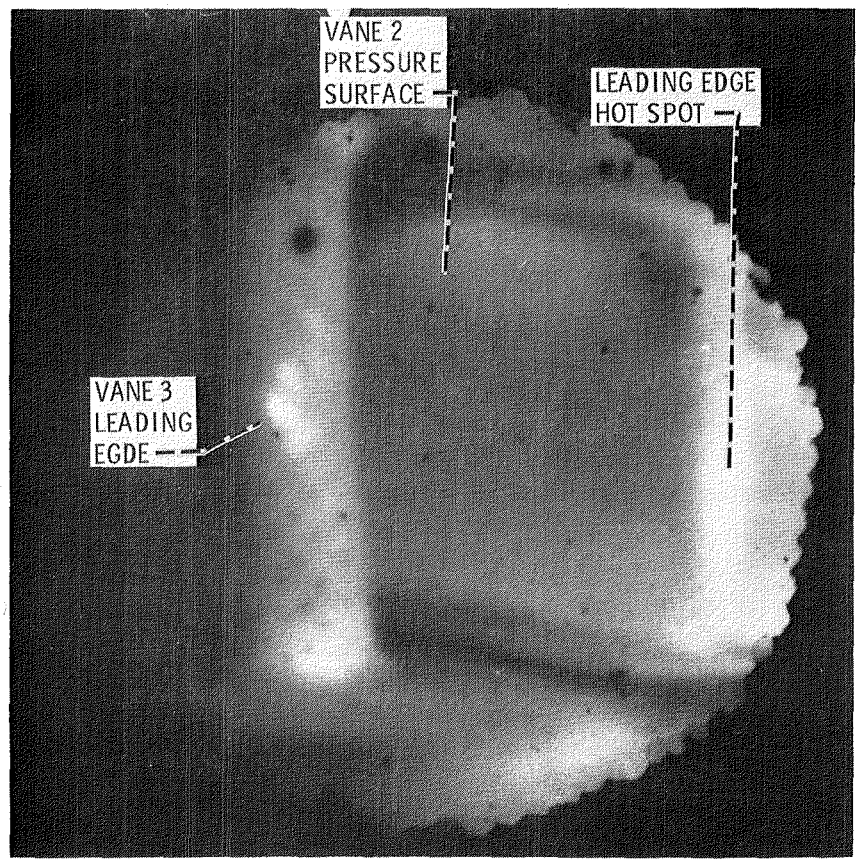

Figure 10. - Thermal image of the leading edge and pressure surface of vane 2 (330^{0} CCW).

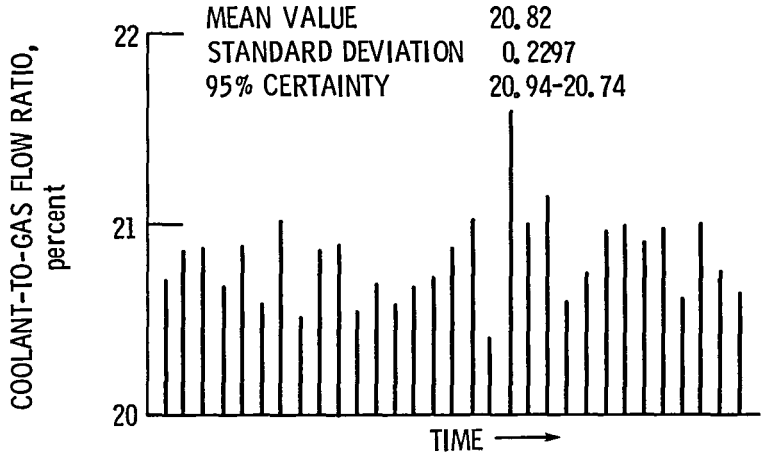

(a) Time history of the coolant-to-gas flow parameter.

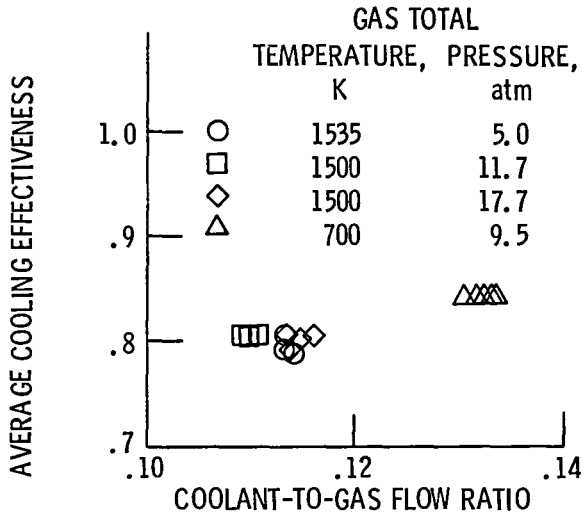

(b) Repeatability of HSF demonstrated by repetitive data taken at a specified set-point.

Figure 11. - Facility operational stability and repeatability.

1. Report No	2 Government Accession No	3 Recipient's Catalog No
NASA TM-86890		

4 Title and Subtitle	5 Report Date
Heat Transfer Results and Operational Characteristics of the NASA Lewis Research Center Hot Section Cascade Test Facility	6 Performing Organization Code: 533-04-1D

7 Author(s)	8 Performing Organization Report No
Herbert J. Gladden, Frederick C. Yeh, and Dennis L. Fronek	E-2357
	10 Work Unit No

9 Performing Organization Name and Address	11 Contract or Grant No
National Aeronautics and Space Administration Lewis Research Center Cleveland, Ohio 44135	
	13 Type of Report and Period Covered: Technical Memorandum
12 Sponsoring Agency Name and Address	14 Sponsoring Agency Code
National Aeronautics and Space Administration Washington, D.C. 20546	

15 Supplementary Notes

Prepared for the Thirtieth International Gas Turbine Conference and Exhibit sponsored by the American Society of Mechanical Engineers, Houston, Texas, March 17-21, 1985.

16 Abstract

The NASA Lewis Research Center gas turbine hot section test facility has been developed to provide a "real-engine" environment with well known boundary conditions for the aerothermal performance evaluation/verification of computer design codes. The initial aerothermal research data obtained at this facility are presented and the operational characteristics of the facility are discussed. This facility is capable of testing at temperatures and pressures up to 1600 K and 18 atm which corresponds to a vane exit Reynolds number range of 0.5×10^6 to 2.5×10^6 based on vane chord. The component cooling air temperature can be independently modulated between 330 and 700 K providing gas-to-coolant temperature ratios similar to current engine application. Research instrumentation of the test components provide conventional pressure and temperature measurements as well as metal temperatures measured by IR-photography. The primary data acquisition mode is steady state through a 704 channel multiplexer/digitizer. The test facility was configured as an annular cascade of full coverage film cooled vanes for the initial series of research tests. These vanes were tested over a wide range of gas Reynolds number, exit gas Mach number and heat flux levels. The range of test conditions was used to represent both actual operating conditions and similarity state conditions of a gas turbine engine. The results are presented for the aerothermal performance of the facility and the full coverage film cooled vanes.

17 Key Words (Suggested by Author(s))	18 Distribution Statement
Heat transfer Film cooling Turbine cooling	Unclassified - unlimited STAR Category 34

19 Security Classif (of this report)	20 Security Classif (of this page)	21 No of pages	22 Price*
Unclassified	Unclassified		

*For sale by the National Technical Information Service, Springfield, Virginia 22161

End of Document